THE APPLICATION OF THE WAVE POTENTIAL FUNCTIONS TO THE ANALYSIS OF TRANSIENT ELECTROMAGNETIC FIELDS

Natalia Georgieva and Yotka Rickard
Department of Electrical and Computer Engineering, McMaster University
1280 Main Street West, Hamilton, ON L8S 4K1, CANADA

ABSTRACT

The time-domain theory of the wave potential functions is applied to the analysis of transient electromagnetic field propagation for the first time. The field is represented in terms of two scalar wave potentials, instead of the six, electric and magnetic, field components. The problem of boundary conditions at dielectric interfaces and at conducting edges is addressed. The current implementation uses finite differences in the 4-D space-time numerical domain.

I. INTRODUCTION

The traditional time-domain differential-equation techniques for the analysis of the electromagnetic (EM) field propagation are based exclusively on Maxwell's representation in terms of the field vectors $\vec{E}$ and $\vec{H}$. This generic theoretical model guarantees robustness and good versatility with respect to the boundary geometry and the homogeneity of the electromagnetic properties of the structure. On the other hand, it is recognized that the system of the four Maxwell's equations is not the most efficient theoretical model from computational point of view, since it requires the calculation of all six field components in the 4-D (time and space) domain. The introduction of the wave potentials in the time-harmonic EM analysis [1] demonstrates the general idea of reducing the number of unknowns from six to two scalar functions, namely the wave potential functions. The price to pay is the increase of the order of the partial differential equations to be solved, since the wave potentials are governed by the second-order wave equation. Besides, the derivation of the two decoupled wave-potential equations implies the homogeneity of the medium, i.e. $\nabla\varepsilon = 0$ and $\nabla\mu = 0$.

In this paper, we present the first results of a novel approach to the treatment of transient EM field problems, namely the time-domain wave potential (TD-WP) approach. This work is closely related to previous research on the time-domain EM field analysis in terms of the magnetic vector potential [2]. The derivation of the wave potential equations is described. Mode coupling at dielectric interfaces and at sharp edges/wedges is also considered in brief. Finally, some numerical test results are shown, which verify the feasibility of the algorithm through comparisons with analytical solutions or numerical (FDTD) simulations.

The algorithm is as versatile as the most popular time-domain techniques (e.g. the Finite-Difference Time-Domain (FDTD) method or the Transmission-Line Matrix (TLM) method) with respect to boundary shapes, since its current implementation is based on finite differences. In the same time, it offers the advantage of full-wave analysis in terms of only two scalar quantities, the magnetic and the electric wave potentials, $A\hat{u}$ and $F\hat{u}$. In the case of mode-coupling discontinuities, the wave equations no longer hold, and mode-coupling equations for the boundary values of A and F must be solved.

II. BASIC EQUATIONS

II.1. Basic concepts in the vector-potential theory of transient EM fields

The vector potentials (VPs) $\vec{A}$ and $\vec{F}$ are introduced into the time-domain EM field analysis in a way, which is essentially the same as in the theory of time-harmonic fields [1]. It is briefly summarized below for the general case of a lossy region.

- $\vec{H}^A = \frac{1}{\mu}\nabla\times\vec{\mathcal{A}}$ $\quad\to\quad$ $\nabla\times\vec{H}^A = \varepsilon\partial_t\vec{E}^A + \sigma\vec{E}^A + \vec{J}$, $\quad -\nabla\times\vec{E}^A = \mu\partial_t\vec{H}^A$

$$\Rightarrow \varepsilon\partial_t\vec{E}^A = \nabla\times\left(\frac{1}{\mu}\nabla\times\vec{\mathcal{A}}\right) - \sigma\vec{E}^A - \vec{J}$$

$$\Rightarrow \vec{E}^A = -\partial_t\vec{\mathcal{A}} - \nabla\phi \qquad (1)$$

- $\vec{E}^F = -\frac{1}{\varepsilon}\nabla\times\vec{\mathcal{F}}$ $\quad\to\quad$ $-\nabla\times\vec{E}^F = \mu\partial_t\vec{H}^F + \sigma_m\vec{H}^F + \vec{M}$, $\quad \nabla\times\vec{H}^F = \varepsilon\partial_t\vec{E}^F$

$$\Rightarrow \mu\partial_t \vec{H}^F = \nabla\times\left(\frac{1}{\varepsilon}\nabla\times\vec{\mathcal{F}}\right) - \sigma_m \vec{H}^F - \vec{M} \qquad (2)$$
$$\Rightarrow \vec{H}^F = -\partial_t \vec{\mathcal{F}} - \nabla\psi$$

The EM field due to the magnetic vector potential $\vec{\mathcal{A}}$ in (1) has a divergence free $\vec{B}^A$ vector, and therefore it has only electric type sources (electric currents $\vec{J}$ and electric charges ρ). The EM field due to the electric vector potential $\vec{\mathcal{F}}$ (2) has a divergence free $\vec{D}^F$ vector, and it can only have magnetic type sources (magnetic currents $\vec{M}$ and magnetic charges ρ_m). The dual character of both fields is apparent. Each vector potential has its scalar complement. Here, ϕ denotes the electric scalar potential, and ψ represents the magnetic scalar potential. For brevity, the derivatives of the first and the second order with respect to the variables (ξ,ζ) are denoted as ($\partial_\xi,\partial_\zeta$) and ($\partial^2_{\xi\xi},\partial^2_{\zeta\zeta}$, or $\partial^2_{\xi\zeta}$), respectively.

The two final equations for $\vec{E}^A$ in (1) and for $\vec{H}^F$ in (2) lead to the governing equations of $\vec{\mathcal{A}}$ and $\vec{\mathcal{F}}$ in their most general form:

$$\nabla\times\left(\frac{1}{\mu}\nabla\times\vec{\mathcal{A}}\right) + \varepsilon\partial^2_{tt}\vec{\mathcal{A}} + \sigma\partial_t\vec{\mathcal{A}} + \varepsilon\nabla\partial_t\phi + \sigma\nabla\phi = \vec{J} \qquad (3)$$

$$\nabla\times\left(\frac{1}{\varepsilon}\nabla\times\vec{\mathcal{F}}\right) + \mu\partial^2_{tt}\vec{\mathcal{F}} + \sigma_m\partial_t\vec{\mathcal{F}} + \mu\nabla\partial_t\psi + \sigma_m\nabla\psi = \vec{M} \qquad (4)$$

The construction of solutions in terms of VPs is based on the superposition of both fields: $(\vec{E}^A,\vec{H}^A)$ and $(\vec{E}^F,\vec{H}^F)$. Note that this implies the linearity of the medium.

There are no general restrictions on the choice of the directions of the VPs $\vec{\mathcal{A}}$ and $\vec{\mathcal{F}}$, as long as this choice ensures fulfillment of the boundary conditions of the EM problem. Besides, from the leftmost relations in (1)-(2), it is obvious that a collinear pair ($\vec{\mathcal{A}},\vec{\mathcal{F}}$) forms a complete set of ($\vec{E},\vec{H}$) fields, in the sense that the $(\vec{E}^A,\vec{H}^A)$ field and the $(\vec{E}^F,\vec{H}^F)$ field are orthogonal with respect to their longitudinal components: $H^A_u = 0 \wedge H^F_u \neq 0$ and $E^A_u \neq 0 \wedge E^F_u = 0$, where $\hat{u}$ denotes the direction of the VP. This takes us one step further to the introduction of the wave potentials (WPs) A and F, which are scalar functions defined as the magnitudes of the collinear vector potentials: $\vec{\mathcal{A}} = A\hat{u}$ and $\vec{\mathcal{F}} = F\hat{u}$. Thus, the description of the EM field in terms of the WPs is in effect a way to represent it as a superposition of two types of modes: the TM_u modes $(\vec{E}^A,\vec{H}^A)$ and the TE_u modes $(\vec{E}^F,\vec{H}^F)$.

II. 2. Homogeneous region

So far, no assumptions were made with regard to the homogeneity of the electric and magnetic properties of the region. The equations (3)-(4) represent the behavior of $\vec{\mathcal{A}}$ and $\vec{\mathcal{F}}$ in the general case of inhomogeneous (but isotropic and linear) medium. They are significantly simplified in the case of a homogeneous region where the conditions $\nabla\varepsilon = 0$ and $\nabla\mu = 0$ hold. The application of the Lorentz' gauge to both equations as:

$$\begin{aligned}\mu\varepsilon\partial_t\phi + \mu\sigma\phi &= -\nabla\cdot\vec{\mathcal{A}}\\ \mu\varepsilon\partial_t\psi + \varepsilon\sigma_m\psi &= -\nabla\cdot\vec{\mathcal{F}}\end{aligned} \qquad (5)$$

reduces them to the following form:

$$\nabla^2\vec{\mathcal{A}} - \mu\varepsilon\partial^2_{tt}\vec{\mathcal{A}} - \mu\sigma\partial_t\vec{\mathcal{A}} = -\mu\vec{J} \qquad (6)$$

$$\nabla^2\vec{\mathcal{F}} - \mu\varepsilon\partial^2_{tt}\vec{\mathcal{F}} - \varepsilon\sigma_m\partial_t\vec{\mathcal{F}} = -\varepsilon\vec{M} \qquad (7)$$

Equations (6)-(7) are decoupled and they hold everywhere except at line or surface sources, and, depending on their direction, at discontinuities such as dielectric interfaces and edges.

Equations (6)-(7) are complemented by the boundary conditions (BC) for A and F. The cases of electric wall and magnetic wall are trivial. They lead to homogeneous BC either of Dirichlet, or of Neumann type. For example, at electric walls, a tangential A vanishes, and a tangential F has a zero normal derivative; a normal A has a zero normal derivative, and a normal F vanishes.

II.3. Dielectric interfaces

A dielectric interface (DI) is a surface (e.g. $x = x_i$ plane), at which the dielectric permittivity has a discontinuity: $\partial\varepsilon/\partial n = (\varepsilon_2 - \varepsilon_1)\,\delta(x - x_i)$. Here, $\hat{n}$ is the surface normal unit vector pointing from region (1) to region (2). It can be easily shown that if the vector potentials' direction $\hat{u}$ is normal to the DI, i.e. $\hat{u} = \pm\hat{n}$, then A and F can satisfy separately the continuity of the tangential field components, $\vec{E}_\tau$ and $\vec{H}_\tau$. The boundary conditions in this case are derived as:

$$A^{(1)} = A^{(2)} \quad , \quad \frac{\partial_n A^{(1)}}{\varepsilon_1} = \frac{\partial_n A^{(2)}}{\varepsilon_2} \qquad (8)$$

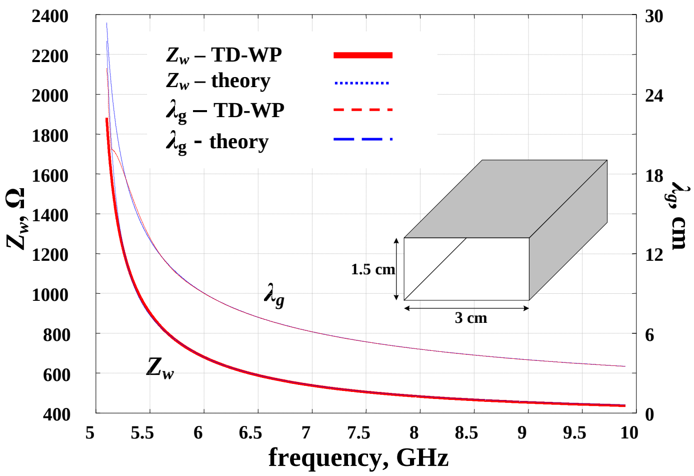

Fig. 1. Wave impedance and guide wavelength of a rectangular waveguide – comparison between TD-WP numerical results with the analytical solution.

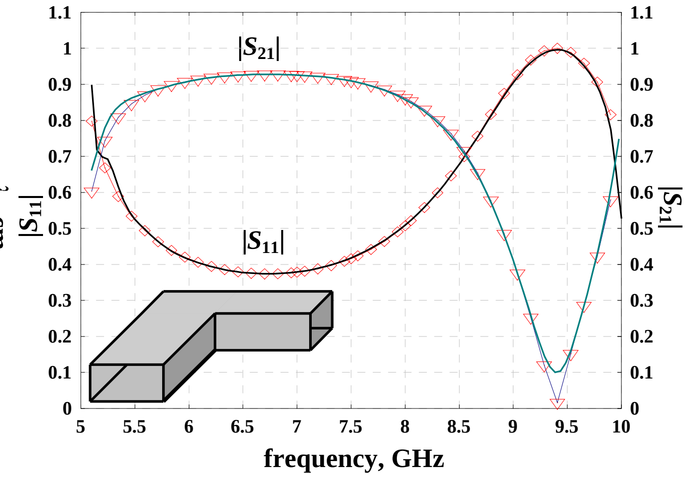

Fig. 2. Magnitudes of the *S*-parameters of the right-angle waveguide bend (*a*=3 cm, *b*=1.5 cm): with lines – TD-WP, with line-points – HP HFSS simulation.

$$\frac{F^{(1)}}{\varepsilon_1}=\frac{F^{(2)}}{\varepsilon_2}\quad,\quad\frac{\partial_n F^{(1)}}{\varepsilon_1}=\frac{\partial_n F^{(2)}}{\varepsilon_2}\tag{9}$$

It is important to note that there is no mode coupling occurring in this case.

When the VPs are tangential to the DI, i.e. $\hat{u}\perp\hat{n}$, A and F cannot satisfy separately the tangential field continuity. Mode coupling takes place because of the mutual dependence of the WPs. Without loss of generality, one can assume that $\hat{n}=\hat{x}$, and $\hat{u}=\hat{z}$. Then, the boundary relations appear as:

$$\partial_{tt}^2\left(A^{(2)}-A^{(1)}\right)=\frac{1}{\mu}\partial_{zz}^2\left(\frac{A^{(2)}}{\varepsilon_2}-\frac{A^{(1)}}{\varepsilon_1}\right)\tag{10}$$

$$\partial_t\left(\partial_x A^{(2)}-\partial_x A^{(1)}\right)=\partial_{yz}^2\left(\frac{F^{(2)}}{\varepsilon_2}-\frac{F^{(1)}}{\varepsilon_1}\right)\tag{11}$$

$$\partial_{tt}^2\left(F^{(2)}-F^{(1)}\right)=\frac{1}{\mu}\partial_{zz}^2\left(\frac{F^{(2)}}{\varepsilon_2}-\frac{F^{(1)}}{\varepsilon_1}\right)\tag{12}$$

$$\partial_t\left(\frac{1}{\varepsilon_2}\partial_x F^{(2)}-\frac{1}{\varepsilon_1}\partial_x F^{(1)}\right)=-\frac{1}{\mu}\partial_{yz}^2\left(\frac{A^{(2)}}{\varepsilon_2}-\frac{A^{(1)}}{\varepsilon_1}\right)\tag{13}$$

II.4. Edges of perfect conductors

Edges represent another type of discontinuity where mode coupling may occur. We shall consider the simplest case of a straight-line edge. If the VP direction $\hat{u}$ is tangential to the edge linear element $\hat{\tau}$, then the WPs are not coupled. This is rather obvious, since $E_\tau^F=E_u^F=0$ is true everywhere; and for $E_\tau^A=0$ to be true, the following boundary relation must be imposed:

$$\partial_t A=-\partial_\tau\phi\tag{14}$$

If the VPs are normal to the edge ($\hat{u}\perp\hat{\tau}$), then coupling will occur because the condition $\vec{E}_\tau=0$ implies mutual dependence of both modes. Assume that $\hat{u}=\hat{x}$ and $\hat{\tau}=\hat{z}$. Then, $\partial_y F=\partial_z\phi$. For example, in a microstrip-line structure, the field can be represented by the WPs corresponding to the VPs, which are normal to the layers. These WPs are coupled only at the strip edge, and they are decoupled at the dielectric interface. An excellent work on mode coupling at strip and corner edges can be found in [3]. This work considers in detail the coupling of modes due to VPs, which are normal to the edges, in spectral domain analysis. However, the general conclusions hold for transient fields, too.

III. RESULTS AND DISCUSSION

We present part of the numerical tests through which the feasibility of the approach and the sources of errors in its finite-difference implementation have been studied.

A. Hollow rectangular waveguide – guide wave-length, wave impedance

This example provides comparison with analytical solutions. The waveguide has a cross-section of dimensions: *a*=3 cm, *b*=1.5 cm ($f_c=5$ GHz). Two simulations were performed: using longitudinal ($\hat{z}$) and vertical ($\hat{x}$) WPs. The results are identical. The numerical results are plotted together with the analytical solution in Fig. 1. The excitation of the waveguide is with a dominant TE_{01}-mode distribution

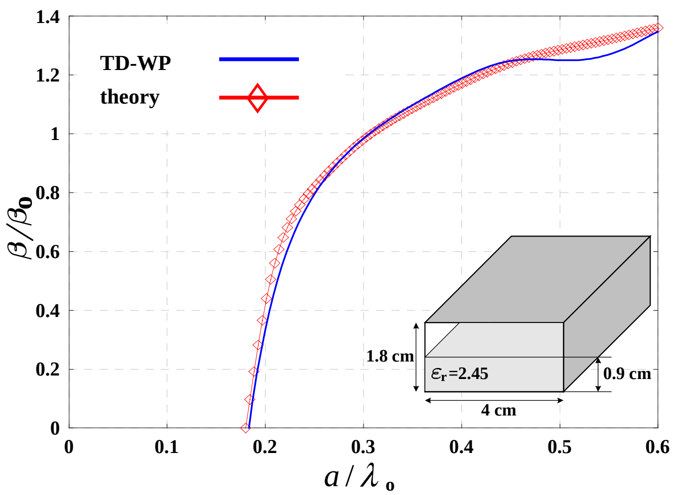

Fig. 3. Normalized phase constant of a partially filled waveguide: with line-points – analytical solution (dominant mode), with line – TD-WP.

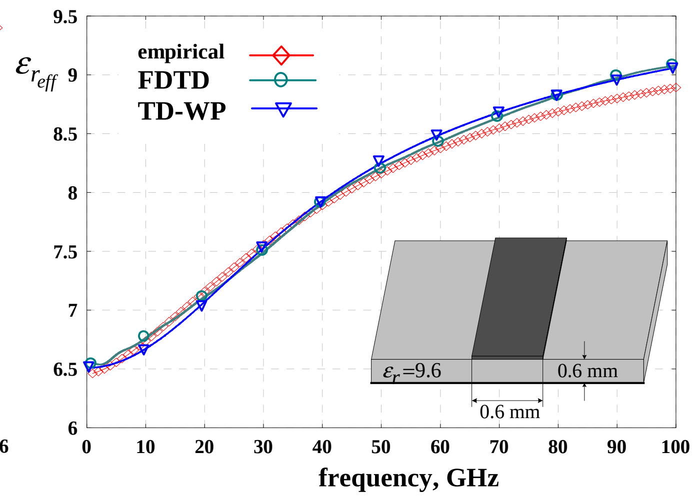

Fig. 4. Dispersion in the effective dielectric constant of a microstrip line – comparison with the empirical formula of Hammerstad-Jensen [6] and with the FDTD results.

of the E_x component whose time waveform is a sine wave modulated by Blackman-Harris window [4].

B. Right-angle H-plane waveguide bend

The two ports of the bend have the same cross-section as in example *A* above. The excitation is in the same frequency band of the dominant mode. The *S*-parameters were calculated and compared with the results of the simulations made with HP HFSS [5] (see Fig. 2).

C. Partially filled waveguide – propagation constant

This example has analytical solution, which can be found in [1]. The waveguide has a cross-section of dimensions: *a*=4 cm, *b*=1.8 cm. It is partially filled with a dielectric layer ($\varepsilon_r = 2.45$) of thickness *h*=0.9 cm. The results in the frequency band of the dominant mode are given in Fig. 3, where the normalized phase constant β/β_0 is plotted vs. the ratio a/λ_0. Here, λ_0 is the wavelength in free space.

C. *Microstrip line – effective dielectric constant*

The effective dielectric constant of a microstrip line was calculated in the frequency range from 0 GHz to 100 GHz. The microstrip is of infinitesimal thickness on a substrate of $\varepsilon_r = 9.6$. The thickness of the substrate is *h*=0.6 mm, and the width of the strip is *w*=0.6 mm. The TD-WP results are plotted in Fig. 4 together with the FDTD simulation output and the empirical formula of Hammerstad and Jensen [6].

CONCLUSIONS

A novel approach to the time-domain analysis of field propagation is presented in this paper based on the time-domain theory of wave potentials. The boundary conditions for the wave potentials have been derived, as well as their mode-coupling relations at dielectric interfaces and edges. The proposed approach is applicable to problems of various boundaries and inhomogeneous regions. It requires the computation of only two scalar quantities in time and space, instead of the six $\vec{E}$ and $\vec{H}$ field components. Thus, it reduces the computational cost of the transient simulations significantly in comparison with the existing differential-equation approaches to time-domain EM modeling such as the FDTD method or the TLM method.

REFERENCES

[1] R.F. Harrington, *Time-Harmonic Electromagnetic Fields*, McGraw-Hill, Inc., New York, 1961.

[2] N. Georgieva and E. Yamashita, “Time-domain vector-potential analysis of transmission line problems,” *IEEE Trans. Microwave Theory and Tech.*, Vol. MTT-46, No 4, pp. 404-410, April 1998.

[3] A.S. Omar and K. Schünemann, “Space-domain decoupling of LSE and LSM fields in generalized planar guiding structures,” *IEEE Trans. Microwave Theory and Tech*., Vol. MTT-32, No 12, pp. 1626-1632, Dec. 1984.

[4] F.J. Harris, “On the use of windows for harmonic analysis with the discrete Fourier transform,” *Proc. IEEE*, Vol. 66, No 1, pp. 51-83, Jan 1978.

[5] HP HFSS™ Version 5.2, 1400 Fountaingrove Parkway, Santa Rosa, CA 95403-1799, 1998.

[6] E. Hammerstad and O. Jensen, “Accurate models for microstrip computer-aided design,” 1980 *IEEE Int. Microwave Symp. Digest*, pp. 407-409, 1980.

Next Paper